Journal of chemical & engineering data

Article

Cite This: J. Chem. Eng. Data XXXX, XXX, XXX−XXX

pubs.acs.org/jced

Simultaneous Determination of All Species Concentrations in Multiequilibria for Aqueous Solutions of Dihydrogen Phosphate Considering Debye−Hückel Theory

Joseph Schell,[†] Ethan Zars,[†] Carmen Chicone,[‡] and Rainer Glaser*[,†]

[†]Department of Chemistry, University of Missouri, Columbia, Missouri 65211, United States

[‡]Department of Mathematics, University of Missouri, Columbia, Missouri 65211, United States

Supporting Information

ABSTRACT: Solutions of citric acid and Na_2HPO_4 were studied with the dynamical approach to multiequilibria systems. This widely employed buffer has a well-defined pH profile and allows for the study of the distribution of phosphate species over a wide pH range. The dynamical approach is a flexible and accurate method for the calculation of all species concentrations in multiequilibria considering ionic strength (I) via Debye−Hückel theory. The agreement between the computed pH profiles and experiment is excellent. The equilibrium concentrations of the non-hydrogen species are reported for over 30 buffer mixtures across the entire pH range. These new concentration data enable researchers to lookup the equilibrium distribution of species at any pH. The data highlight the dramatic effects of ionic strength, and for example, the position of maximal $H_2PO_4^-$ concentration is shifted by almost an entire pH unit! From a more general perspective, the study allows for a discussion of the dependence of concentration quotients Q_{xy} on ionic strength, $pQ_{xy} = f(I)$, and for the numerical demonstration that the thermodynamic equilibrium constants $K_{xy,act}(I) = K_{xy}$. The analysis emphasizes the need for measurements of the concentrations of several species in complex multiequilibria systems over a broad pH range to advance multiequilibria simulations.

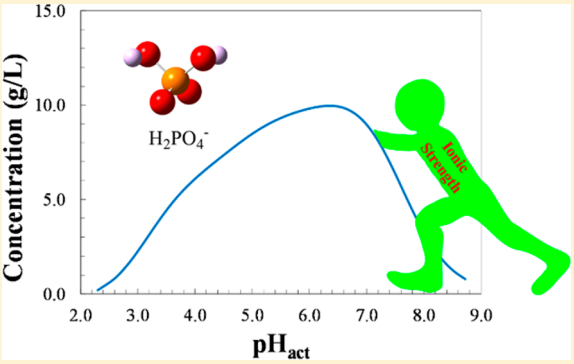

1. INTRODUCTION

Systems of polyprotic acids/bases inherently involve complex equilibria. Given the pH of an acid−base system at equilibrium, the concentration of each ionic species present in solution can be deduced via the solution of a polynomial.[1,2] Generally, the order of the polynomial grows with the number of species in the acid−base equilibrium and the mathematical solution can become rather complex. Similar computations for a buffer system involving one or more polyprotic species are more complicated, and it is even more challenging to determine the concentration of each species when the effect of the ionic strength (I) of the solution is considered. Tessman and Ivanov developed software to calculate the pH of a given mixture by solution of the nth degree, single-variable polynomial with consideration of ionic strength, and the results agreed with experiment.[3] Numerical methods also have since been developed for the calculation of all equilibrium species using the *Solver* tool in Microsoft Excel.[4,5]

In previous work, we described the dynamical approach for the simultaneous solution of all species concentrations for multi-equilibria systems of mixtures of acids and their conjugate bases.[6,7] The dynamical approach entails the numerical solution of a set of first-order ordinary differential equations (ODEs) derived from the chemical equilibria expressions. This approach offers significant advantages including the ability to easily treat complex systems and the facile incorporation of Debye−Hückel theory.[7] Importantly, the approach maintains a straightforward mathematical description of the multiequilibria system, which requires only basic knowledge of mass action kinetic theory.

The present study extends the dynamical approach to include equilibrium problems with several multiply charged species. Our previous study of the pH profile of the NaOH titration of citric acid showed that the effects of ionic strength can be very large, especially for the highly charged species.[7] It therefore seemed prudent to explore mixtures that contain a larger number of highly charged species. The buffer system comprised of citric acid (H_3Cit) and dibasic sodium phosphate (Na_2HPO_4) was selected because it is a widely employed buffer system with a well-defined pH profile over a wide range of pH values. Moreover, it allows one to study the distribution of phosphate species in aqueous solution over a wide pH range. We compare our results to the experimental data sets by McIlvaine[8] and Sigma-Aldrich[9] and demonstrate that the dynamical approach is a convenient, flexible, and accurate method for the calculation of all species in complex acid/base equilibria at various acidities and ionic strengths. The calculated pH profile simulates the experimental data with resounding agreement. We also report the equilibrium

Received: February 16, 2018
Accepted: May 11, 2018

DOI: 10.1021/acs.jced.8b00146
J. Chem. Eng. Data XXXX, XXX, XXX−XXX

concentrations of the non-hydrogen species and discuss the effects of ionic strength on the equilibrium distribution. Experimentally, the concentrations of these species are seldom reported because of the inherent difficulty in their measurements. With the concentrations of these other species as a function of pH, researchers are able to quickly and easily determine the optimal pH for a desired equilibrium species distribution. From a more theoretical perspective, the computed concentrations of all species allow for a discussion of concentration quotients and their dependence on ionic strength. Moreover, the approaches described in the present paper will be useful to studies of ionic strength dependence of equilibria in general.[10−13]

2. PHOSPHATE RECOVERY EFFORTS AND $H_2PO_4^-$-SELECTIVE MOLECULAR SENSORS

The citric acid/phosphate buffer systems present an excellent opportunity to study the pH dependence of phosphate concentrations in aqueous solution. Phosphates are essential nutrients for all life, and often, they are the limiting nutrient in soil for plant growth. Using mined phosphates to fertilize the soil is rapidly exhausting the supply of phosphate available.[14,15] On the other hand, overuse of phosphate fertilizers and the inability to recycle them have caused eutrophication in natural waters.[16,17] Thus, efforts have been made to recover phosphates from wastewater and solid biowaste.[14,18−20] Recovery of phosphate from aqueous solutions via adsorption by activated alumina,[21] Gd complexes,[22] Fe−Mn binary colloids,[23] iron oxide tailings,[24] crab shells,[25] red mud,[26] steel slag,[27] oxygen furnace slag,[28] and ferric sludge[29] has been shown to be pH dependent. A doubly beneficial reaction to sequester aluminum(III) with phosphate has also recently been shown to be pH and ionic strength dependent.[30]

Electrochemical[31,32] and optical[33,34] sensors for phosphate have also been explored. It is well-known that proteins selectively bind anions, including phosphates, in specific protonation states.[35−37] Many of the optical sensors that have been developed are based on this protein chemistry. Some examples of well characterized $H_2PO_4^-$ receptors are illustrated in Supporting Information (Figure S1), and these include $H_2PO_4^-$ binding using amides and pyridines with a ferrocenoyl scaffold,[38] bis-ureas,[39] tetraamides together with pyridines,[40,41] bis-indoles with pyridines,[42] amides and ethers,[43] and sapphyrins.[44] The anion recognition studies require high-accuracy concentration measurements to determine accurate complexation constants.[45] Thus, knowledge of the equilibrium distribution of phosphate species becomes essential for the determination of these complexation constants in aqueous media.

3. METHODS: DYNAMICAL APPROACH TO EQUILIBRIUM CONCENTRATIONS

Debye−Hückel theory and its variants[46,47] are the most common approach to approximate activity coefficients of ions in electrolyte solutions. To account for nonideal dynamical behavior of ionic species in solution, the concentrations of the ionic species are replaced with activities a_i in the kinetic equations. The activity a_i of the ith species S_i with absolute charge z is calculated via eq 1. In principle, the units of $[S_i]$ can be any concentration unit (molal, molar) and we used molar concentrations, which are required as initial conditions in the ODEs.

$$a_i = f_z[S_i^z] \tag{1}$$

$$\log_{10}(f_z) = Az^2\left(\frac{\sqrt{I}}{1+\sqrt{I}} - bI\right) \tag{2}$$

$$I = 0.5\sum_i z_i^2[S_i] \tag{3}$$

The activity coefficients, f_z, were calculated using the Davies approximation[48] to Debye−Hückel theory (eq 2). The coefficient $A = e^2B/(2.3038\pi\varepsilon_0\varepsilon_r kT)$, where e is the electron charge, ε is the static dielectric constant of water, k is the Boltzmann constant, T is temperature, and $B = (2e^2N_L/\varepsilon_0\varepsilon_r kT)^{1/2}$.[49,50] At room temperature, A has an approximate value of 0.5108 $kg^{1/2}$ $mol^{-1/2}$ and B is approximately 0.3287×10^8 $kg^{1/2}$ cm^{-1} $mol^{-1/2}$.[50−52] The Davies approximation includes the empirical parameter b with a static value for all ions. Davies' original work assigns $b = 0.2$, and this value was shown to give improved activity coefficients for large anions at low ionic strength based on conductivity measurements.[48] However, the parameter $b = 0.1$ also has been used in some studies for pH profiles.[7,53] In this work, we report the results obtained using both $b = 0.1$ and $b = 0.2$. The ionic strength was calculated via eq 3. Included in eq 3 are all of the species participating in the kinetic equations and the cations contributed by the added salts. The counterion concentrations are constant and equal to the respective initial anion concentrations. The Davies equation is believed to give a possible error of 3% at $I = 0.1$ mol L^{-1} and 10% at $I = 0.5$ mol L^{-1}.[51]

For a buffer system of a triprotic acid, H_3A, and the salt of a second triprotic acid, $(M^+)_n(H_{3-n}B^{n-})$, the system of equilibria and their equilibrium equations are as follows:

$$H_2O \rightleftarrows H^+ + OH^- \quad K_w = a(H^+)a(OH^-) \tag{4}$$

$$H_3A \rightleftarrows H^+ + H_2A^- \quad K_{11} = a[H^+]a[H_2A^-]/a[H_3A] \tag{5}$$

$$H_2A^- \rightleftarrows H^+ + HA^{2-} \quad K_{12} = a[H^+]a[HA^{2-}]/a[H_2A^-] \tag{6}$$

$$HA^{2-} \rightleftarrows H^+ + A^{3-} \quad K_{13} = a[H^+]a[A^{3-}]/a[HA^{2-}] \tag{7}$$

$$H_3B \rightleftarrows H^+ + H_2B^- \quad K_{21} = a[H^+]a[H_2B^-]/a[H_3B] \tag{8}$$

$$H_2B^- \rightleftarrows H^+ + HB^{2-} \quad K_{22} = a[H^+]a[HB^{2-}]/a[H_2B^-] \tag{9}$$

$$HB^{2-} \rightleftarrows H^+ + B^{3-} \quad K_{23} = a[H^+]a[B^{3-}]/a[HB^{2-}] \tag{10}$$

The equilibrium constants are given as K_{xy}, where x denotes the identity of the acid and y is the dissociation number. For citric acid (H_3Cit, 2-hydroxypropane-1,2,3-tricarboxylic acid) at room temperature, the pK_a value of the carboxyl group attached to C2 is 3.13 and the pK_a values for the second and third dissociations are 4.76 and 6.40.[54] The pK_a values of phosphoric acid at room temperature are 2.16, 7.21, and 12.32.[54,55] Note that the dynamical method can be employed at other temperatures with the consideration of the temperature dependence of the equilibrium constants via the van't Hoff equation. The ionic strength dependence of the pK_a values of various acids has been studied, and in solutions with ionic strengths below 0.6, the changes to the above pK_a values are less than 0.3 for both citric acid and phosphoric acid.[56]

The equilibria of eqs 4−10 lead to the following kinetic differential equations according to general mass action kinetics:[57−59]

DOI: 10.1021/acs.jced.8b00146
J. Chem. Eng. Data XXXX, XXX, XXX−XXX

Table 1. Reported and Calculated pH Values and Ionic Strengths for a Series of Mixtures[a] of the Buffer Solution

			expt.[8]	$f = 1$		$b = 0.1$		$b = 0.2$		lit.[b]	ionic strength		
mix.	$[H_3Cit]_0$ (g/L)	$[HPO_4^{2-}]_0$ (g/L)	pH	pH_{conc}	pH_{act}	pH_{conc}	pH_{act}	pH_{conc}	pH_{act}	pH_{act}	$f = 1$	$b = 0.1$	$b = 0.2$
1	18.83	0.38	2.2	2.25	2.30	2.18	2.23	2.18	2.23	2.23	0.01	0.01	0.01
2	18.02	1.19	2.4	2.53	2.60	2.41	2.48	2.41	2.48	2.48	0.03	0.03	0.03
3	17.12	2.09	2.6	2.77	2.86	2.61	2.70	2.61	2.70	2.70	0.05	0.05	0.05
4	16.17	3.04	2.8	3.00	3.10	2.80	2.90	2.80	2.90	2.90	0.07	0.07	0.07
5	15.26	3.94	3.0	3.21	3.32	2.98	3.09	2.99	3.09	3.09	0.08	0.09	0.09
6	14.47	4.74	3.2	3.41	3.53	3.15	3.26	3.16	3.27	3.26	0.10	0.10	0.10
7	13.74	5.47	3.4	3.63	3.75	3.32	3.45	3.34	3.45	3.45	0.12	0.12	0.12
8	13.03	6.18	3.6	3.89	4.01	3.51	3.64	3.53	3.66	3.64	0.14	0.14	0.14
9	12.39	6.81	3.8	4.15	4.28	3.70	3.84	3.73	3.86	3.84	0.15	0.16	0.16
10	11.81	7.40	4.0	4.40	4.53	3.89	4.03	3.92	4.05	4.03	0.17	0.17	0.17
11	11.26	7.95	4.2	4.63	4.77	4.07	4.22	4.11	4.25	4.22	0.19	0.19	0.19
12	10.74	8.47	4.4	4.87	5.01	4.26	4.41	4.31	4.44	4.41	0.21	0.21	0.21
13	10.23	8.97	4.6	5.13	5.27	4.47	4.62	4.52	4.66	4.62	0.23	0.23	0.23
14	9.74	9.46	4.8	5.42	5.57	4.69	4.85	4.75	4.89	4.85	0.25	0.25	0.25
15	9.32	9.89	5.0	5.70	5.84	4.90	5.06	4.96	5.11	5.06	0.27	0.27	0.27
16	8.91	10.29	5.2	5.93	6.08	5.09	5.26	5.17	5.32	5.26	0.29	0.29	0.29
17	8.50	10.70	5.4	6.14	6.29	5.29	5.46	5.37	5.52	5.46	0.31	0.31	0.31
18	8.07	11.13	5.6	6.33	6.48	5.49	5.66	5.57	5.73	5.66	0.33	0.33	0.33
19	7.60	11.60	5.8	6.51	6.66	5.69	5.86	5.78	5.93	5.86	0.35	0.35	0.35
20	7.08	12.12	6.0	6.68	6.83	5.89	6.06	5.98	6.13	6.06	0.37	0.37	0.37
21	6.51	12.69	6.2	6.84	7.00	6.08	6.25	6.16	6.32	6.25	0.39	0.39	0.39
22	5.91	13.29	6.4	7.00	7.15	6.24	6.42	6.33	6.49	6.42	0.41	0.41	0.41
23	5.24	13.96	6.6	7.15	7.31	6.41	6.59	6.50	6.65	6.59	0.43	0.43	0.43
24	4.37	14.83	6.8	7.34	7.50	6.59	6.78	6.69	6.85	6.78	0.46	0.46	0.46
25	3.39	15.81	7.0	7.55	7.71	6.80	6.98	6.90	7.06	6.98	0.49	0.49	0.49
26	2.51	16.69	7.2	7.75	7.92	7.00	7.19	7.11	7.27	7.19	0.52	0.52	0.52
27	1.76	17.44	7.4	7.96	8.13	7.21	7.39	7.32	7.48	7.39	0.54	0.55	0.54
28	1.22	17.98	7.6	8.16	8.32	7.40	7.59	7.51	7.67	7.59	0.56	0.56	0.56
29	0.82	18.38	7.8	8.36	8.52	7.59	7.78	7.71	7.87	7.78	0.57	0.57	0.57
30	0.53	18.67	8.0	8.56	8.72	7.80	7.99	7.91	8.08	7.99	0.58	0.58	0.58

[a]Volumes of buffer solutions given in ref 8 were converted to concentrations (g/L). *I* reported in mol/L. [b]Calculated using the method described in ref 5 (see the Supporting Information).

$$\frac{d[H^+]}{dt} = k_{11f}[H_3A] - f_1^2 k_{11b}[H^+][H_2A^-] + f_1 k_{12f}[H_2A^-] - f_1 f_2 k_{12b}[H^+][HA^{2-}] + f_2 k_{13f}[HA^{2-}] - f_1 f_3 k_{13b}[H^+][A^{3-}] + k_{21f}[H_3B] - f_1^2 k_{21b}[H^+][H_2B^-] + f_1 k_{22f}[H_2B^-] - f_1 f_2 k_{22b}[H^+][HB^{2-}] + f_2 k_{23f}[HB^{2-}] - f_1 f_3 k_{23b}[H^+][B^{3-}] + k_{wf} - f_1^2 k_{wb}[H^+][OH^-] \quad (11)$$

$$\frac{d[H_3A]}{dt} = f_1^2 k_{11b}[H^+][H_2A^-] - k_{11f}[H_3A] \quad (12)$$

$$\frac{d[H_2A^-]}{dt} = f_1 f_2 k_{12b}[H^+][HA^{2-}] - f_1 k_{12f}[H_2A^-] + k_{11f}[H_3A] - f_1^2 k_{11b}[H^+][H_2A^-] \quad (13)$$

$$\frac{d[HA^{2-}]}{dt} = f_1 f_3 k_{13b}[H^+][A^{3-}] - f_2 k_{13f}[HA^{2-}] + f_1 k_{12f}[H_2A^-] - f_1 f_2 k_{12b}[H^+][HA^{2-}] \quad (14)$$

$$\frac{d[A^{3-}]}{dt} = f_2 k_{13f}[HA^{2-}] - f_1 f_3 k_{13b}[H^+][A^{3-}] \quad (15)$$

$$\frac{d[H_3B]}{dt} = f_1^2 k_{21b}[H^+][H_2B^-] - k_{21f}[H_3B] \quad (16)$$

$$\frac{d[H_2B^-]}{dt} = f_1 f_2 k_{22b}[H^+][HB^{2-}] - f_1 k_{22f}[H_2B^-] + k_{21f}[H_3B] - f_1^2 k_{21b}[H^+][H_2B^-] \quad (17)$$

$$\frac{d[HB^{2-}]}{dt} = f_1 f_3 k_{23b}[H^+][B^{3-}] - f_2 k_{23f}[HB^{2-}] + f_1 k_{22f}[H_2B^-] - f_1 f_2 k_{22b}[H^+][HB^{2-}] \quad (18)$$

$$\frac{d[B^{3-}]}{dt} = f_2 k_{23f}[HB^{2-}] - f_1 f_3 k_{23b}[H^+][B^{3-}] \quad (19)$$

$$\frac{d[OH^-]}{dt} = k_{wf} - f_1^2 k_{wb}[H^+][OH^-] \quad (20)$$

The method calls for the assignment of the forward reaction rate constants (k_f), the backward reaction rate constants (k_b), and the initial concentrations. One significant advantage of the dynamical approach is that the species concentrations are all described as functions of time, which theoretically allows for the

DOI: 10.1021/acs.jced.8b00146
J. Chem. Eng. Data XXXX, XXX, XXX−XXX

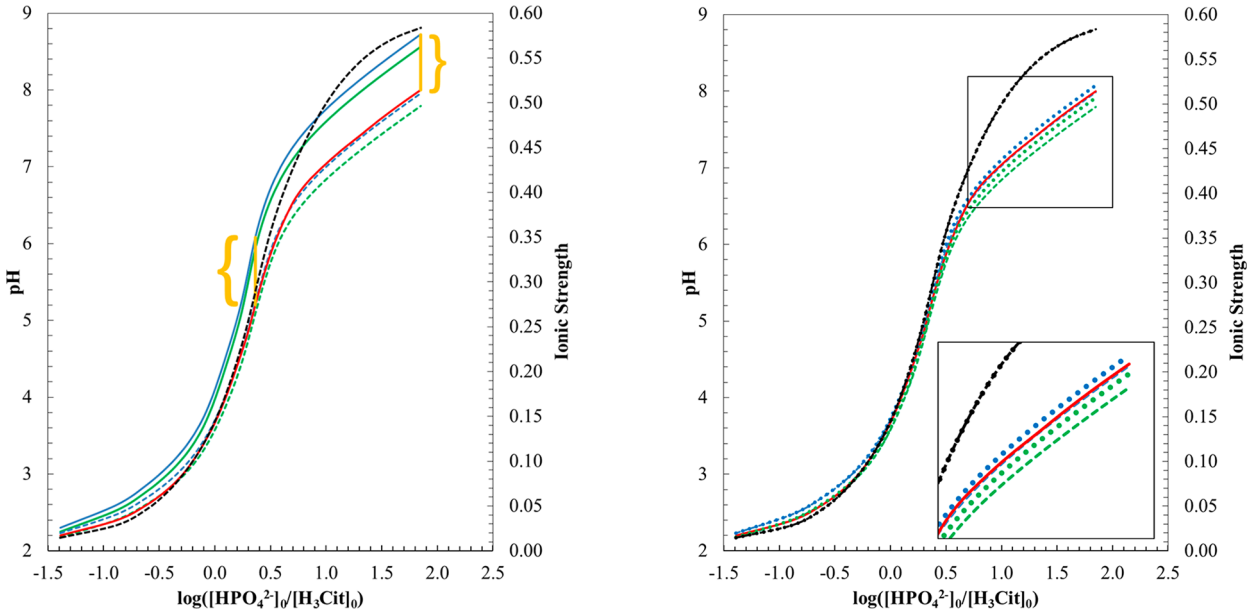

Figure 1. Comparison of experimental pH values (red curve, ref 8) to pH values computed with various methods (blue and green curves). The black line shows the ionic strength of the solution and is plotted with respect to the secondary axis. Solid lines show pH values calculated with $f = 1$, and dashed lines represent pH values calculated with the Davies approximation with $b = 0.1$. Blue curves indicate pH_{act}, and green curves indicate pH_{conc}. The orange lines and indicators show the deviation between the $f = 1$, pH_{act} curve (solid, blue) and experiment for two mixtures in different regions of the pH profile. On the right, the experimental pH values are compared to pH values computed with $b = 0.1$ (dashed lines) and $b = 0.2$ (dotted lines).

approximation of species concentrations far from equilibrium if accurate values of the forward and backward rate constants, k_f and k_b, are known.[60−63] However, since we are primarily concerned with equilibrium, the k_f values were arbitrarily set to 10^2 for all reactions and the respective k_b values were determined by $K = k_f/k_b$. Since K_{xy} is fixed, k_{xyf} could be assigned any numerical value and the equilibrium concentration data would be unchanged because k_{xyb} is defined algebraically; varying k_{xyf} only affects the time at which equilibrium is reached. The system of ODEs was solved with the *NDSolve*[64] utility in *Mathematica*.[65] The resulting functions were evaluated for the interval $0 \leq t \leq 1$ s, and plots of the species concentrations with respect to time were generated to ensure equilibrium had been established.

The data set by McIlvaine[8] covers a broader pH range than the data reported by Sigma-Aldrich,[9] and we discuss the results for the former and report the results for the latter in the Supporting Information. For simplicity of comparison with experiment, we converted the volumes of dibasic sodium phosphate and citric acid given in the experimental work to concentrations; these appear in columns 2 and 3 of Table 1 in g/L. In the Supporting Information, Table S1 is a reproduction of Table 1 with these concentrations in mol/L, as they are used in the ODEs. The experimentally measured pH values are listed in column 4 of Table 1.

4. RESULTS AND DISCUSSION

4.1. pH Calculation with the Dynamical Method. Three sets of equilibrium concentrations were computed for each buffer mixture. One set corresponds to an ideal system, where the ionic strength of the solution is considered to have no effect on equilibrium concentrations (i.e., $f = 1$). The other two sets include the effects of ionic strength using activity coefficients calculated with the Davies[48] equation with $b = 0.1$ or $b = 0.2$. The ionic strengths of the equilibrium solutions were calculated for all three data sets, and they appear in the last three columns of Table 1.

Electrometric measurements of H^+ concentrations correspond to the activity of H^+ rather than its concentration.[66] We calculated pH values using both concentrations and activities and refer to them as pH_{conc} and pH_{act}, respectively; $pH_{conc} = -\log[H^+]$ and $pH_{act} = -\log[a(H^+)]$. Therefore, six values of pH were determined for each buffer mixture and they are shown in columns 5−10 of Table 1: pH_{conc} and pH_{act} for $f = 1$ and pH_{conc} and pH_{act} values calculated using the Davies approximation with $b = 0.1$ and $b = 0.2$, respectively.

The experimental data[8] are compared to the calculated pH values in Figure 1. The ratio $\log([HPO_4^{2-}]_0/[H_3Cit]_0)$ is used as the independent variable to achieve a compact axis that uses relative concentrations of HPO_4^{2-} and H_3Cit such that any mixture of these two will fit within a small plot window. As the ratio increases, the solution becomes more basic and the ionic strength increases (secondary axis in Figure 1, black curve).

Figure 1 illustrates that ionic strength greatly affects pH. The pH values calculated with $f = 1$ (solid curves) show large deviations from the experimental pH over the entire range of mixtures with an average error of 9.1 and 11.9% for pH_{conc} and pH_{act}, respectively. Note that the deviation between the computed pH_{act} values and the experimental pH corresponds to the *vertical* distance between the two curves at a given value of $\log([HPO_4^{2-}]_0/[H_3Cit]_0)$. A first inspection of Figure 1 might suggest that the deviation is largest in the region $\log([HPO_4^{2-}]_0/[H_3Cit]_0) > 1$ (average error of 9.5%). However, the largest deviations actually occur in the region $0.0 < \log([HPO_4^{2-}]_0/[H_3Cit]_0) < 0.1$ (average error of 14.7%). In fact, deviations are large even at very low ionic strengths with a 10.0% error at $I = 0.05$ M. Orange indicators were added to Figure 1 (left) to clearly illustrate this deviation.

The agreement between experiment and the data calculated with Debye−Hückel theory and $b = 0.1$ (dashed curves in Figure 1) is a magnitude better with average errors of only 2.1 and 1.1% for pH_{conc} and pH_{act}, respectively. The resounding agreement between experiment and the computed pH_{act} data gets even

DOI: 10.1021/acs.jced.8b00146
J. Chem. Eng. Data XXXX, XXX, XXX−XXX

Table 2. Calculated Citrate Species Concentrations[a] at Equilibrium for the Series of Mixtures of Buffer Solution

	[H_3Cit]			[H_2Cit^-]			[$HCit^{2-}$]			[Cit^{3-}]		
mix.	$f = 1$	$b = 0.1$	$b = 0.2$	$f = 1$	$b = 0.1$	$b = 0.2$	$f = 1$	$b = 0.1$	$b = 0.2$	$f = 1$	$b = 0.1$	$b = 0.2$
1	16.637	16.462	16.465	2.173	2.343	2.341	0.007	0.010	0.010	0.000	0.000	0.000
2	14.382	14.230	14.234	3.599	3.739	3.735	0.021	0.032	0.032	0.000	0.000	0.000
3	11.842	11.737	11.741	5.195	5.269	5.267	0.053	0.083	0.082	0.000	0.000	0.000
4	9.231	9.188	9.189	6.782	6.757	6.758	0.117	0.185	0.182	0.000	0.000	0.000
5	6.834	6.870	6.869	8.157	7.985	7.993	0.228	0.362	0.356	0.000	0.001	0.001
6	4.817	4.952	4.945	9.186	8.823	8.842	0.411	0.636	0.625	0.000	0.002	0.002
7	3.121	3.369	3.355	9.829	9.245	9.277	0.726	1.058	1.040	0.001	0.005	0.005
8	1.744	2.080	2.060	9.896	9.142	9.186	1.316	1.724	1.700	0.004	0.014	0.013
9	0.888	1.216	1.195	9.190	8.473	8.519	2.229	2.596	2.573	0.012	0.034	0.032
10	0.427	0.672	0.654	7.868	7.355	7.393	3.399	3.622	3.607	0.034	0.078	0.074
11	0.197	0.350	0.337	6.248	5.975	5.998	4.651	4.685	4.683	0.079	0.165	0.157
12	0.083	0.168	0.159	4.559	4.503	4.509	5.838	5.656	5.672	0.171	0.325	0.310
13	0.029	0.070	0.065	2.922	3.056	3.046	6.821	6.389	6.428	0.365	0.621	0.598
14	0.008	0.025	0.023	1.586	1.841	1.819	7.283	6.643	6.700	0.766	1.134	1.101
15	0.002	0.009	0.008	0.819	1.061	1.038	7.018	6.332	6.395	1.378	1.815	1.775
16	0.001	0.003	0.003	0.422	0.578	0.561	6.262	5.593	5.655	2.127	2.636	2.591
17	0.000	0.001	0.001	0.219	0.292	0.283	5.274	4.571	4.635	2.904	3.532	3.476
18	0.000	0.000	0.000	0.115	0.136	0.134	4.246	3.453	3.527	3.605	4.372	4.301
19	0.000	0.000	0.000	0.059	0.058	0.058	3.267	2.407	2.490	4.172	5.027	4.944
20	0.000	0.000	0.000	0.029	0.024	0.024	2.406	1.576	1.657	4.546	5.377	5.296
21	0.000	0.000	0.000	0.014	0.010	0.010	1.708	1.003	1.071	4.697	5.404	5.335
22	0.000	0.000	0.000	0.007	0.004	0.004	1.181	0.635	0.687	4.634	5.179	5.128
23	0.000	0.000	0.000	0.003	0.002	0.002	0.779	0.391	0.427	4.375	4.762	4.726
24	0.000	0.000	0.000	0.001	0.001	0.001	0.447	0.211	0.233	3.857	4.092	4.070
25	0.000	0.000	0.000	0.000	0.000	0.000	0.222	0.100	0.112	3.116	3.238	3.226
26	0.000	0.000	0.000	0.000	0.000	0.000	0.105	0.046	0.052	2.363	2.422	2.416
27	0.000	0.000	0.000	0.000	0.000	0.000	0.046	0.020	0.022	1.684	1.711	1.708
28	0.000	0.000	0.000	0.000	0.000	0.000	0.021	0.009	0.010	1.180	1.192	1.191
29	0.000	0.000	0.000	0.000	0.000	0.000	0.009	0.004	0.004	0.795	0.800	0.799
30	0.000	0.000	0.000	0.000	0.000	0.000	0.004	0.001	0.002	0.516	0.519	0.518

[a]Concentrations in g/L. Data computed for the mixtures listed in Table 1.

better with increasing I, especially in the region $x > 0$. The pH_{conc} values agree with experiment better than pH_{act} only at very low ionic strength ($I < 0.1$).

The graph on the right side of Figure 1 compares the experimental pH values to the pH_{conc} (green) and pH_{act} (blue) values computed with $b = 0.1$ (dashed) and $b = 0.2$ (dotted). Relative to the $b = 0.1$ values, the computed $b = 0.2$ data sets shift to higher pH at higher ionic strength. The pH_{act} values are overestimated and in slightly worse agreement than their $b = 0.1$ counterparts with 1.7% error with respect to experimental values. However, the pH_{conc} values still fall below the experimental pH curve and are in better agreement than the pH_{conc} values for $b = 0.1$ with an average error of 1.1%. The lower error of pH_{conc} values is due to the strong agreement in the region of low ionic strength. For $I < 0.25$, the $b = 0.2$ curves behave the same as $b = 0.1$ and yield very similar pH values. The ionic strength is shown for both $b = 0.1$ and $b = 0.2$, and they agree with each other for all mixtures.

4.2. Calculation of All Species Concentrations at Equilibrium with the Dynamical Method. A major advantage of the dynamical approach is that the equilibrium concentrations of all species in the system are obtained simultaneously. Table 2 shows the concentrations (in g/L) of H_3Cit, H_2Cit^-, $HCit^{2-}$, and Cit^{3-} (top), and Table 3 shows the concentrations of H_3PO_4, $H_2PO_4^-$, HPO_4^{2-}, and PO_4^{3-} at equilibrium for each mixture. The computations require the specification of concentrations in units of mol/L, and the results are given in mmol/L in Table S2a and b. Again, these values are reported for both the $f = 1$ data set and the data sets with activity considerations.

Figure 2 shows the non-H^+ species concentrations as functions of pH_{act}. The H_nCit^{n-3} and $H_mPO_4^{m-3}$ species are plotted on the top and bottom, respectively. The plots in Figure 2 show that the concentration maxima occur at significantly different pH values for the $f = 1$ (solid) and Davies (dashed) data sets. Since the $b = 0.1$ and $b = 0.2$ data sets give exactly the same curves, only the $b = 0.1$ data set is shown in Figure 2.

The H_3Cit concentration starts at about 16 g/L for the most acidic solution studied and decreases as the fraction of HPO_4^{2-} increases. As the solution becomes more basic, one observes maxima for the concentrations of the conjugate bases: [H_2Cit^-] at pH ≈ 4.0 ($f = 1$) or 3.4 (Davies), [$HCit^{2-}$] at pH ≈ 5.6 ($f = 1$) or 4.8 (Davies), and [Cit^{3-}] at pH ≈ 7.0 ($f = 1$) or 6.2 (Davies).

High concentrations of HPO_4^{2-} occur at high pH. Even at the most basic pH values studied, only a small fraction of HPO_4^{2-} is deprotonated. Thus, the [PO_4^{3-}] curve essentially lies on the pH_{act} axis and [PO_4^{3-}] never reaches 0.01 g/L. As the fraction of citric acid increases, the pH decreases and HPO_4^{2-} is protonated. The concentration of $H_2PO_4^-$ is highest at pH ≈ 6.4 ($f = 1$) or 5.6 (Davies). Further protonation of $H_2PO_4^-$ occurs only to a small extent, and $H_2PO_4^-$ remains the dominant $H_mPO_4^{m-3}$ species in solution. The concentration of neutral H_3PO_4 only goes through a shallow maximum at pH ≈ 2.9 ($f = 1$) or 2.7 (Davies).

DOI: 10.1021/acs.jced.8b00146
J. Chem. Eng. Data XXXX, XXX, XXX−XXX

Table 3. Calculated Phosphate Species Concentrations[a] at Equilibrium for the Series of Mixtures of Buffer Solution

	$[H_3PO_4]$			$[H_2PO_4^-]$			$[HPO_4^{2-}]$			$[PO_4^{3-}]$		
mix.	$f = 1$	$b = 0.1$	$b = 0.2$	$f = 1$	$b = 0.1$	$b = 0.2$	$f = 1$	$b = 0.1$	$b = 0.2$	$f = 1$	$b = 0.1$	$b = 0.2$
1	0.176	0.168	0.168	0.214	0.222	0.222	0.000	0.000	0.000	0.000	0.000	0.000
2	0.363	0.351	0.351	0.843	0.856	0.855	0.000	0.000	0.000	0.000	0.000	0.000
3	0.418	0.410	0.410	1.701	1.709	1.708	0.000	0.000	0.000	0.000	0.000	0.000
4	0.394	0.393	0.393	2.685	2.685	2.685	0.000	0.000	0.000	0.000	0.000	0.000
5	0.330	0.338	0.338	3.659	3.651	3.651	0.000	0.001	0.001	0.000	0.000	0.000
6	0.256	0.273	0.272	4.537	4.520	4.520	0.001	0.001	0.001	0.000	0.000	0.000
7	0.183	0.209	0.207	5.346	5.319	5.321	0.001	0.002	0.002	0.000	0.000	0.000
8	0.116	0.149	0.147	6.128	6.094	6.096	0.003	0.004	0.004	0.000	0.000	0.000
9	0.071	0.105	0.102	6.810	6.775	6.777	0.006	0.007	0.007	0.000	0.000	0.000
10	0.043	0.073	0.070	7.423	7.393	7.395	0.011	0.013	0.013	0.000	0.000	0.000
11	0.027	0.050	0.048	7.982	7.959	7.961	0.021	0.022	0.022	0.000	0.000	0.000
12	0.017	0.034	0.032	8.499	8.483	8.484	0.038	0.038	0.038	0.000	0.000	0.000
13	0.010	0.022	0.021	8.984	8.979	8.980	0.074	0.066	0.067	0.000	0.000	0.000
14	0.005	0.014	0.013	9.404	9.428	9.427	0.152	0.120	0.123	0.000	0.000	0.000
15	0.003	0.009	0.008	9.691	9.773	9.767	0.293	0.206	0.212	0.000	0.000	0.000
16	0.002	0.006	0.005	9.873	10.044	10.031	0.517	0.343	0.357	0.000	0.000	0.000
17	0.001	0.004	0.003	9.959	10.238	10.215	0.845	0.566	0.590	0.000	0.000	0.000
18	0.001	0.002	0.002	9.936	10.315	10.281	1.300	0.923	0.958	0.000	0.000	0.000
19	0.000	0.001	0.001	9.780	10.217	10.175	1.925	1.491	1.533	0.000	0.000	0.000
20	0.000	0.001	0.001	9.464	9.892	9.850	2.756	2.332	2.374	0.000	0.000	0.000
21	0.000	0.001	0.000	8.977	9.341	9.306	3.804	3.444	3.479	0.000	0.000	0.000
22	0.000	0.000	0.000	8.337	8.618	8.592	5.042	4.764	4.790	0.000	0.000	0.000
23	0.000	0.000	0.000	7.528	7.727	7.708	6.515	6.318	6.336	0.000	0.000	0.000
24	0.000	0.000	0.000	6.390	6.511	6.500	8.505	8.385	8.396	0.000	0.000	0.000
25	0.000	0.000	0.000	5.022	5.084	5.078	10.838	10.776	10.782	0.000	0.000	0.000
26	0.000	0.000	0.000	3.744	3.774	3.771	12.985	12.955	12.958	0.000	0.001	0.001
27	0.000	0.000	0.000	2.639	2.654	2.652	14.827	14.812	14.813	0.001	0.002	0.001
28	0.000	0.000	0.000	1.838	1.846	1.845	16.156	16.147	16.149	0.001	0.003	0.002
29	0.000	0.000	0.000	1.234	1.239	1.238	17.157	17.149	17.150	0.002	0.004	0.004
30	0.000	0.000	0.000	0.802	0.807	0.806	17.871	17.862	17.864	0.003	0.007	0.006

[a]Concentrations in g/L. Data computed for the mixtures listed in Table 1.

Figure 2 demonstrates in a compelling fashion the importance of ionic strength on the distribution of species at equilibrium. The positions of the maxima of the solid ($f = 1$) and dashed (Davies) curves can be separated by almost an entire pH unit! The concentration of any species typically decreases rapidly as the pH shifts away from the pH value where the species' concentration is highest. Hence, small differences in pH can have drastic effects on the equilibrium distribution of a non-H^+ species.

Numerical data for the specific cases at pH 4.7 and 6.3 are provided in Table 4. The last column in Table 4 shows the percentage change and the direction of the change of the concentration of species S associated with inclusion of the activity effects; $\Delta = 100\cdot([S, b = 0.1] - [S, f = 1])/(0.5\cdot([S, b = 0.1] + [S, f = 1]))$. Wide discrepancies are apparent for the two models, and the percent differences, Δ, range from 14.3 to 200.0%. Clearly, the inclusion of ionic strength effects is vital to the accurate determination of equilibrium species distribution at a given pH.

A second practical application of Figure 2 concerns the determination of the optimal pH to achieve a relative maximum of a desired ionic species. For example, the $f = 1$ curve in Figure 2 would suggest that the optimum pH to maximize $[H_2PO_4^-]$ would be 6.5. However, when ionic strength effects are included, one finds that at pH 6.5 the concentration of the $H_2PO_4^-$ ion would only be about 75% of the maximum value and the solution would have approximately a 1:3 ratio of $[HPO_4^{2-}]/[H_2PO_4^-]$. The appropriate pH to maximize $[H_2PO_4^-]$ and diminish interference from its conjugate base is 5.4, as given by the Davies curve. Conversely, to directly compare the ability of a receptor to selectively bind $[H_2PO_4^-]$ over $[HPO_4^{2-}]$, one should select a pH where both of these species exist in similar quantities. An appropriate pH for such a measurement would not be 7.5, as suggested by the $f = 1$ curve, but 6.8, as suggested by the Davies curve.

4.3. Ionic Strength Dependence of Concentration Quotients Q_{xy} and Thermodynamic Equilibrium Constants $K_{xy,act}$. Generally, for the yth dissociation of an m-protic acid H_mA, the concentration quotient Q_y is given by eq 21. In more concentrated solutions, eq 21 needs to be replaced by the corresponding expression for the thermodynamic equilibrium constants $K_{y,act}$ (eq 22) in which all concentrations $[S]$ are replaced by activities $a(S)$.

$$Q_y = [H^+][H_{m-y}A^{-y}]/[H_{m-y+1}A^{1-y}] \tag{21}$$

$$K_{y,act} = f_1[H^+]a(H_{m-y}A^{-y})/a(H_{m-y+1}A^{1-y}) \tag{22}$$

$$K_y = \lim_{I\to 0} Q_y \tag{23}$$

$$K_y = K_{y,act} \quad \text{for} \quad \text{all} \quad I \tag{24}$$

DOI: 10.1021/acs.jced.8b00146
J. Chem. Eng. Data XXXX, XXX, XXX−XXX

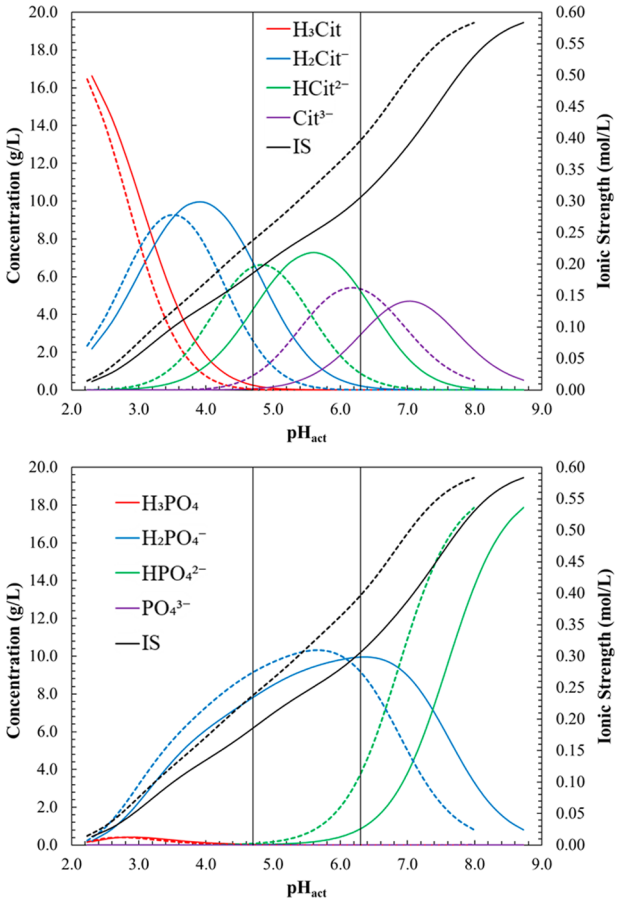

Figure 2. Species concentrations as a function of pH_{act}. The color of the line designates the identity of the species (see legend). Concentrations calculated without ionic strength considerations ($f = 1$) are shown as solid lines, and those calculated with the activity coefficients from the Davies equation with $b = 0.1$ are shown as dashed lines. The black curves show the ionic strength of the equilibrium solutions and are plotted with respect to the secondary axis.

Table 4. Concentration Differences (g/L) for $f = 1$ and Davies Data at Select pH Values

	species, S	$[S, f = 1]$	$[S, b = 0.1]$	Δ (%)
pH 4.7	H_2Cit^-	6.50	2.68	−83.3
	$HCit^{2-}$	4.37	6.46	+38.6
	Cit^{3-}	0.00	0.95	+200.0
	$H_2PO_4^-$	7.86	9.31	+16.9
pH 6.3	$HCit^{2-}$	5.32	1.14	−129.4
	Cit^{3-}	2.65	5.29	+66.7
	$H_2PO_4^-$	10.18	8.83	−14.3
	HPO_4^-	1.06	4.32	+121.4

$$D = A\left(\frac{\sqrt{I}}{1+\sqrt{I}} - bI\right) \tag{25}$$

Inserting eq 2 into eq 22 and using the abbreviation of eq 25, one arrives at eq 26 which relates the concentration quotient Q_y to the thermodynamic equilibrium constant $K_{y,act}$.

$$K_{y,act} = Q_y \cdot \{10^{(2y \cdot D)}\} \tag{26}$$

At infinite dilution, activities and concentrations become equal and the equilibrium coefficient K_y equals the concentration quotient Q_y (eq 23). It is well established that the concentration quotients Q_y do *not* equal K_y even at low ionic strength.[47,67] However, all of the calculations employ the numerical value of K_y for all I. It is a direct consequence of this practice that eq 24 must hold for all I, that is, that the equilibrium constants K_y equal the thermodynamic equilibrium constants $K_{y,act}$ not just in the limit of infinite dilution but in the entire range of ionic strength being modeled with Debye−Hückel theory.

$$Q_{1y} = [H^+][H_{3-y}A^{-y}]/[H_{4-y}A^{1-y}] \tag{27a}$$

$$Q_{2y} = [H^+][H_{3-y}B^{-y}]/[H_{4-y}B^{1-y}] \tag{27b}$$

$$K_{1y,act} = f_1[H^+]a(H_{3-y}A^{-y})/a(H_{4-y}A^{1-y}) \tag{28a}$$

$$K_{2y,act} = f_1[H^+]a(H_{3-y}B^{-y})/a(H_{4-y}B^{1-y}) \tag{28b}$$

Previously, we plotted the concentration quotients Q_{xy} for two systems (acetate-buffered acetic acid; titration of citric acid with sodium hydroxide) using several approximations of Debye−Hückel theory and showed that pQ_y is always less than pK_y and that the difference between them increases nonlinearly as the ionic strength increases.[7] Ganesh et al. recently reported a similar finding for a universal buffer system.[68] We show an example of this kind of plot in Figure S2 of the Supporting Information for the first dissociation of citric acid in the buffer system.

The concentration quotients Q_{xy} were computed for all of the equilibria in the buffer system using eqs 27a and 27b and the concentrations in Table 2. Figure 3 shows the pQ_{xy} curves as functions of ionic strength for citric acid ($x = 1$, left) and phosphoric acid ($x = 2$, right). As before, red horizontal lines show the pK_{xy} values at infinite dilution. The pQ_{xy} curves for all data always are less than the pK_{xy} values at infinite dilution. The difference grows nonlinearly as I increases, as expected, and the deviation always is larger for the $b = 0.1$ data (solid curves) than for the $b = 0.2$ data (dashed curves) for these systems. Also, for any given ionic strength, the difference between the equilibrium constants and the concentration quotients $pK_{xy} - pQ_{xy}$ increases from the first dissociation ($y = 1$), to the second dissociation ($y = 2$), and again to the third dissociation ($y = 3$). This trend is also expected because the z^2 dependency of the f values is more pronounced in the curves of the higher order dissociations.

We also calculated the thermodynamic equilibrium constants $K_{xy,act}(I)$ using eqs 28a and 28b with the concentrations from Table 2 and the activity coefficients from the Davies equation for both $b = 0.1$ and $b = 0.2$, and the results are included in Figure 3 as blue marks. These $pK_{xy,act}(I)$ values all align with the pK_{xy} values at infinite dilution (red lines). This outcome of the numerical solution of the ODE systems is required by eq 24, and Figure 3 thus validates the numerical accuracy of the dynamical approach to multiequilibria system.

4.4. Attempted Speciation of Citric Acid via ^{1}H NMR Spectroscopy. The geminal hydrogens of the two equivalent CH_2 groups are diastereotopic, and the AB spin system gives rise to two doublets with the same coupling constant $^2J_{AB}$.[69] We measured the ^{1}H NMR spectra of a dilute aqueous solution of potassium citrate (5.36 mg of K_3Cit in 100 mL of H_2O) as a function of pH by adding small aliquots of 3 M H_2SO_4. Spectra were recorded on a 600 MHz Bruker Avance III spectrometer using water suppression techniques, and a typical spectrum is shown in the Supporting Information together with a table of the chemical shifts of the four peaks at each pH (Figure S3 and Table S5). The doublets show $^2J = 15.3 \pm 0.4$ Hz, and the chemical

DOI: 10.1021/acs.jced.8b00146
J. Chem. Eng. Data XXXX, XXX, XXX−XXX

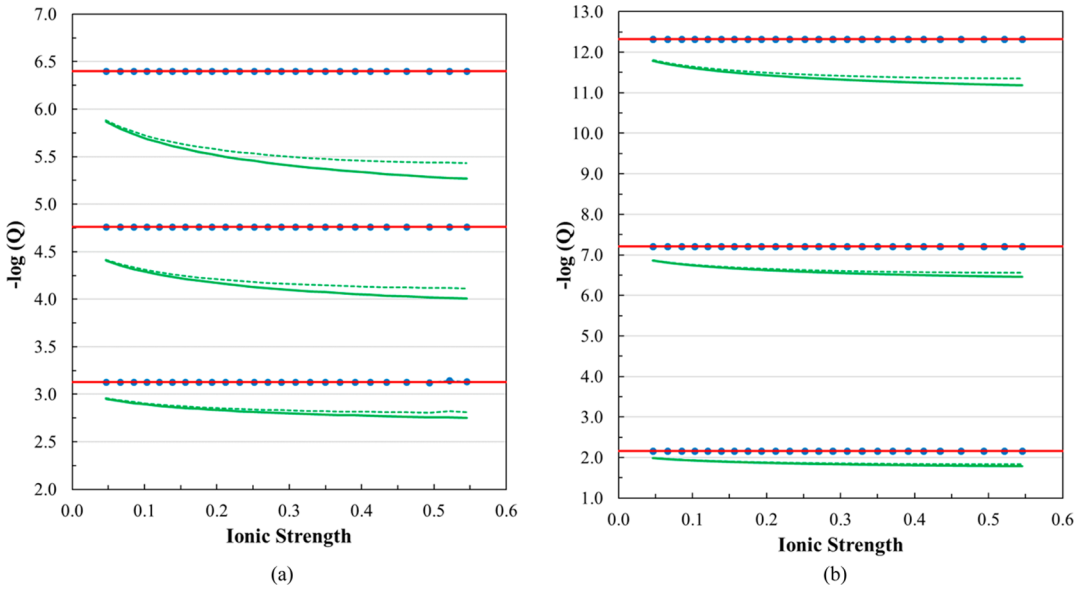

Figure 3. Comparison of the equilibrium coefficient expressions (eqs 21 and 22) for the dissociations of (a) citric acid and (b) phosphoric acid in the mixtures. Line color distinguishes between $pK_{xy,conc}$ (green), $pK_{xy,act}$ (blue), and pK_{xy} (red). Solid, b = 0.1; dashed, b = 0.2. The $pK_{xy,act}$ lines are also marked with circles for improved visibility.

shifts of the centers of the doublets are shown in Figure 4 as a function of pH.

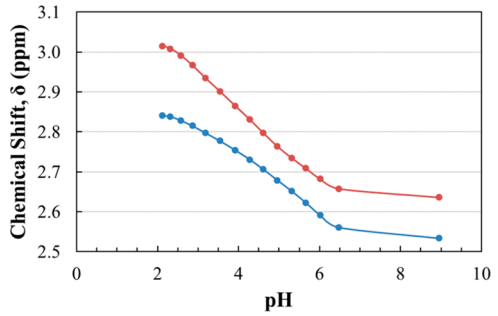

Figure 4. ^{1}H NMR shifts relative to DSS (4,4-dimethyl-4-silapentane-1-sulfonic acid) for citric acid in 90% H_2O:10% D_2O over the pH range 2−9.

Each apparent methylene proton signal δ_H corresponds to the average of the chemical shifts of all protonation states of the species in solution, and a first approximation of δ_H is given by the equation

$$\delta_H = \sum_{i=0}^{3} c_i \times \delta_H(H_iCit^{i-3}) \quad (29)$$

where c_i are the concentration fractions of the species i and $\delta_H(H_iCit^{i-3})$ are the chemical shifts of the respective methylene-H of the individual species. If this equation holds and if the $\delta_H(H_iCit^{i-3})$ values are known, then one should be able to obtain speciation information from eq 29 (i.e., the c_i values). Values for the individual chemical shifts $\delta_H(H_3Cit)$ and $\delta_H(Cit^{3-})$ can be determined experimentally by adding excess acid to an aqueous citrate solution. The $\delta_H(H_3Cit)$ values for the two diastereotopic hydrogens are 2.84 (A) and 3.01 ppm (B), and the $\delta_H(Cit^{3-})$ values are 2.53 (A) and 2.63 ppm (B), respectively (Figure 4). However, the individual shifts $\delta(H_2Cit^-)$ and $\delta(HCit^{2-})$ cannot be determined in "pure" solutions of the respective anions. Instead of gaining reliable speciation information from the chemical shift measurements, the best one can hope for is an additional constraint in a simultaneous fitting process of pH = $f(c_i)$ and of $\delta_H = f(c_i)$ with a given theoretical model for the treatment of the electrolyte solution that includes the values $\delta(H_2Cit^-)$ and $\delta(HCit^{2-})$ as variables. In any case, such attempts cannot be expected to fully succeed because eq 29 assumes that the chemical shift $\delta_H(H_iCit^{i-3})$ of each species is independent of pH and the changing chemical environment. However, in related studies, we and others found that pH effects on chemical shifts can be quite large (up to 0.1 ppm).[70]

4.5. Further Applications and Desiderata. The simulations of the pH profiles (Figure 1) show that the b = 0.1 data achieve the best match with experiment. It would be desirable to assess the quality of a specific Debye−Hückel approximation not just on the concentration of *one* species (pH) but on the concentration dependence of *several* species. This seems particularly well advised in cases where the only measured species is present in very low concentration. From our perspective, it would be highly desirable and instructive to simulate complex multiequilibria systems for which the concentrations of *several* species were measured simultaneously and over a broad pH range. Ideally, the measured species should include systems containing multiply charged ions in significant concentrations.

In the present study, we employed equilibrium constants at infinite dilution K_{xy} and the Davies equation with two discrete b values. Comparison of computed and measured pH values then suggested which b value resulted in better agreement. If one had experimental data for more species, i.e., some of the ions $H_{3-y}A^{-y}$ and $H_{3-y}B^{-y}$ in the present example, then one would have much tougher constraints on the precise formulation of the DH approximation. Moreover, instead of using $K_{xy,\infty} \neq f(I)$, one would also be in a position to explore effects of $K_{xy,act}$ via iterative setting of $K_{xy,act} = f(I)$ together with the determination of the activity coefficients (eq 2) in the process of solving the ODEs. In the range $0 \leq I \leq 0.6$, changes of the pK_a values up to 0.29 and 0.25 units were reported for citric acid and phosphoric acid,

DOI: 10.1021/acs.jced.8b00146
J. Chem. Eng. Data XXXX, XXX, XXX−XXX

respectively,[56] and these data inform about the shape of trial functions $K_{xy,act} = f(I)$. For the present case, Figure 2 (bottom) suggests that precise measurements of $[HCit^{2-}]$ and pH in the range $4 \leq pH \leq 6.5$ would allow one to test such approaches and their effects on the shape of the $[H_2PO_4^-] = f(pH)$ curves.

One further application of the dynamical approach is the indirect determination of accurate binding constants, K_b, for specific ion receptors in aqueous media.[14,30] The dynamical method allows for the facile inclusion of receptor terms $R[t]$ and $RIA[t]$ to describe the concentrations of the receptor and the receptor−ion aggregate, respectively. With these additions, a simple comparison to the experimental pH profile would allow one to estimate the K_b for the receptor. Such a simple determination of binding constants would be invaluable to studies where direct observation of the aggregating species concentrations is difficult or impossible. Even in cases where direct determination of the formation constant is possible, this approach may facilitate the study of the ionic strength dependence of K_b.

5. CONCLUSION

The dynamical approach was employed to describe the complex multiequilibria buffer system of citric acid and disodium hydrogen phosphate, and the experimental pH profile was modeled with astounding accuracy. The effects of ionic strength were shown to be highly important for the calculation of the pH, and the model suggests that the non-H^+ species concentrations are affected by ionic strength effects to an even greater extent. We presented a few examples of common scenarios where neglecting the ionic strength effects would drastically effect the equilibrium species distribution and, therefore, knowledge of the extent of ionic strength effects is essential. We also presented an application for the dynamical approach in the indirect determination of binding constants as functions of ionic strength, which has an immediate and practical use for researchers developing new chemical sensors.

Improvement to the dynamical approach could involve concomitant improvements to approximations of Debye−Hückel theory. The Davies approximation was tested here with the empirical parameters $b = 0.1$ and $b = 0.2$, and we have shown that the $b = 0.1$ data matches more closely with experiment. This can be extended to other approximations, such as the Pitzer equation,[46,71] to see if increased accuracy is attained in the calculation of $[H^+]$. We note that experimental data sets in which concentration profiles for two or more species are monitored would greatly enhance the confidence in the results obtained with the dynamical approach and thereby provide an excellent system to systematically test the extensions to Debye−Hückel theory.

■ ASSOCIATED CONTENT

Supporting Information

The Supporting Information is available free of charge on the ACS Publications website at DOI: 10.1021/acs.jced.8b00146.

A figure illustrating $H_2PO_4^-$ specific receptors (Figure S1), tables containing the complete results computed for the data set Sigma (Tables S3 and S4), a comparison of the numerical accuracy of the dynamical approach and the equilibrium method, and results of the ^1H NMR studies of citric acid (Figure S3 and Table S5) (PDF)

■ AUTHOR INFORMATION

Corresponding Author

*E-mail: GlaserR@missouri.edu.

ORCID

Rainer Glaser: 0000-0003-3673-3858

Funding

This research was supported by NSF-PRISM grant *Mathematics and Life Sciences* (MLS, #0928053). Acknowledgement is made to the donors of the American Chemical Society Petroleum Research Fund (PRF-53415-ND4) and to the National Science Foundation (CHE 0051007) for partial support of this research.

Notes

The authors declare no competing financial interest.

■ REFERENCES

(1) Weltin, E. Calculating Equilibrium Concentrations for Stepwise Binding of Ligands and Polyprotic Acid-Base Systems: A General Numerical Method to Solve Multistep Equilibrium Problems. *J. Chem. Educ.* **1993**, *70*, 568−571.

(2) Harris, D. C. *Quantitative Chemical Analysis*, 8th ed.; W. H. Freeman and Company: New York, 2010; pp 194−197.

(3) Tessman, A. B.; Ivanov, A. V. Computer Calculations of Acid-Base Equilibria in Aqueous Solutions Using the Acid-Base Calculator Program. *J. Anal. Chem.* **2002**, *57*, 2−7.

(4) Baeza-Baeza, J. J.; García-Álvarez-Coque, M. C. Systematic Approach to Calculate the Concentration of Chemical Species in Multi-Equilibrium Problems. *J. Chem. Educ.* **2011**, *88*, 169−173.

(5) Baeza-Baeza, J. J.; García-Álvarez-Coque, M. C. Systematic Approach for Calculating the Concentrations of Chemical Species in Multiequilibrium Problems: Inclusion of the Ionic Strength Effects. *J. Chem. Educ.* **2012**, *89*, 900−904.

(6) Glaser, R. E.; Delarosa, M. A.; Salau, A. O.; Chicone, C. Dynamical Approach to Multiequilibria Problems for Mixtures of Acids and Their Conjugated Bases. *J. Chem. Educ.* **2014**, *91*, 1009−1016.

(7) Zars, E.; Schell, J.; Delarosa, M. A.; Chicone, C.; Glaser, R. Dynamical Approach to Multi-Equilibria Problems Considering the Debye-Hückel Theory of Electrolyte Solutions: Concentration Quotients as a Function of Ionic Strength. *J. Solution Chem.* **2017**, *46*, 643−662.

(8) McIlvaine, T. C. A Buffer Solution for Colorimetric Comparison. *J. Biol. Chem.* **1921**, *49*, 183−186.

(9) Sigma-Aldrich Buffer Reference Center. http://www.sigmaaldrich.com/life-science/core-bioreagents/biological-buffers/learning-center/buffer-reference-center.html#citric (accessed Nov 10, 2017).

(10) De Stefano, C.; Milea, D.; Sammartano, S. Speciation of Phytate Ion in Aqueous Solution. Protonation Constants in Tetraethylammonium Iodide and Sodium Chloride. *J. Chem. Eng. Data* **2003**, *48*, 114−119.

(11) Gianguzza, A.; Pettignano, A.; Sammartano, S. Interaction of the Dioxouranium(VI) Ion with Aspartate and Glutamate in $NaCl_{(aq)}$ at Different Ionic Strengths. *J. Chem. Eng. Data* **2005**, *50*, 1576−1581.

(12) Gharib, F.; Nik, F. S. Ionic Strength Dependence of Formation Constants: Complexation of Dioxovanadium(V) with Tyrosine. *J. Chem. Eng. Data* **2004**, *49*, 271−275.

(13) Bretti, C.; Majlesi, K.; De Stefano, C.; Sammartano, S. Thermodynamic Study on the Protonation and complexation of GLDA with Ca^{2+} and Mg^{2+} at Different Ionic Strengths and Ionic Media at 298.15 K. *J. Chem. Eng. Data* **2016**, *61*, 1895−1903.

(14) Gilbert, N. The Disappearing Nutrient. *Nature* **2009**, *461*, 716−718.

(15) Cordell, D.; Drangert, J.-O.; White, S. The Story of Phosphorus: Global Food Security and Food for Thought. *Global Environ. Change* **2009**, *19*, 292−305.

(16) Oelkers, E. H.; Valsami-Jones, E. Phosphate Mineral Reactivity and Global Sustainability. *Elements* **2008**, *4*, 83−87.

DOI: 10.1021/acs.jced.8b00146
J. Chem. Eng. Data XXXX, XXX, XXX−XXX

(17) Nur, T.; Johir, M. A. H.; Loganathan, P.; Nguyen, T.; Vigneswaran, S.; Kandasamy, J. Phosphate Removal from Water Using an Iron Oxide Impregnated Strong Base Anion Exchange Resin. *J. Ind. Eng. Chem.* **2014**, *20*, 1301−1307.
(18) Lei, Y.; Song, B.; van der Weijden, R. D.; Saakes, M.; Buisman, C. J. N. Electrochemical Induced Calcium Phosphate Precipitation: Importance of Local pH. *Environ. Sci. Technol.* **2017**, *51*, 11156−11164.
(19) Gu, Y.; Xie, D.; Ma, Y.; Qin, W.; Zhang, H.; Wang, G.; Zhang, Y.; Zhao, H. Size Modulation of Zirconium-Based Metal Organic Frameworks for Highly Efficient Phosphate Remediation. *ACS Appl. Mater. Interfaces* **2017**, *9*, 32151−32160.
(20) Huang, R.; Fang, C.; Lu, X.; Jiang, R.; Tang, Y. Transformation of Phosphorus during (Hydro)thermal Treatments of Solid Biowastes: Reaction Mechanisms and Implications for P Reclamation and Recycling. *Environ. Sci. Technol.* **2017**, *51*, 10284−10298.
(21) Neufeld, R. D.; Thodos, G. Removal of Orthophosphates from Aqueous Solutions with Activated Alumina. *Environ. Sci. Technol.* **1969**, *3*, 661−667.
(22) Harris, S. M.; Nguyen, J. T.; Pailloux, S. L.; Mansergh, J. P.; Dresel, M. J.; Swanholm, T. B.; Gao, T.; Pierre, V. C. Gadolinium Complex for the Catch and Release of Phosphate from Water. *Environ. Sci. Technol.* **2017**, *51*, 4549−4558.
(23) Zhang, G.; Liu, H.; Liu, R.; Qu, J. Removal of Phosphate from Water by Fe-Mn binary Adsorbent. *J. Colloid Interface Sci.* **2009**, *335*, 168−174.
(24) Zeng, L.; Li, X.; Liu, J. Adsorptive Removal of Phosphate from Aqueous Solutions Using Iron Oxide Tailings. *Water Res.* **2004**, *38*, 1318−1326.
(25) Jeon, D. J.; Yeom, S. H. Recycling Wasted Biomaterial, Crab Shells, as an Adsorbent for the Removal of High Concentration of Phosphate. *Bioresour. Technol.* **2009**, *100*, 2646−2649.
(26) Huang, W.; Wang, S.; Zhu, Z.; Li, L.; Yao, X.; Rudolph, V.; Haghseresht, F. Phosphate Removal from Wastewater Using Red Mud. *J. Hazard. Mater.* **2008**, *158*, 35−42.
(27) Xiong, J.; He, Z.; Mahmood, Q.; Liu, D.; Yang, X.; Islam, E. Phosphate Removal from Solution Using Steel Slag through Magnetic Separation. *J. Hazard. Mater.* **2008**, *152*, 211−215.
(28) Xue, Y.; Hou, H.; Zhu, S. Characteristics and Mechanisms of Phosphate Adsorption onto Basic Oxygen Furnace Slag. *J. Hazard. Mater.* **2009**, *162*, 973−980.
(29) Song, X.; Pan, Y.; Wu, Q.; Cheng, Z.; Ma, W. Phosphate Removal from Aqueous Solutions by Adsorption Using Ferric Sludge. *Desalination* **2011**, *280*, 384−390.
(30) Aiello, D.; Cardiano, P.; Cigala, R. M.; Gans, P.; Giacobello, F.; Giuffrè, O.; Napoli, A.; Sammartano, S. Sequestering Ability of Oligophosphate Ligands toward Al^{3+} in Aqueous Solutions. *J. Chem. Eng. Data* **2017**, *62*, 3981−3990.
(31) Kolliopoulos, A. V.; Kampouris, D. K.; Banks, C. E. Rapid and Portable Electrochemical Quantification of Phosphorus. *Anal. Chem.* **2015**, *87*, 4269−4274.
(32) Busschaert, N.; Caltagirone, C.; Rossom, W. V.; Gale, P. A. Applications of Supramolecular Anion Recognition. *Chem. Rev.* **2015**, *115*, 8038−8155.
(33) Hargrove, A. E.; Nieto, S.; Zhang, T.; Sessler, J. L.; Anslyn, E. V. Artificial Receptors for the Recognition of Phosphorylated Molecules. *Chem. Rev.* **2011**, *111*, 6603−6782.
(34) Molina, P.; Zapata, F.; Caballero, A. Anion Recognition Strategies Based on Combined Noncovalent Interactions. *Chem. Rev.* **2017**, *117*, 9907−9972.
(35) Mangani, S.; Ferraroni, M. In *Supramolecular Chemistry of Anions*; Bianchi, A., Bowman-James, K., García-España, E., Eds.; Wiley-VCH: New York, 1997; Chapter 3, pp 63−78.
(36) Hirsch, A. K. H.; Fischer, F. R.; Diederich, F. Phosphate Recognition in Structural Biology. *Angew. Chem., Int. Ed.* **2007**, *46*, 338−352.
(37) Schaly, A.; Belda, R.; García-España, E.; Kubik, S. Selective Recognition of Sulfate Anions by a Cyclopeptide-Derived Receptor in Aqueous Phosphate Buffer. *Org. Lett.* **2013**, *15*, 6238−6241.
(38) Beer, P. D.; Graydon, A. R.; Johnson, A. O.; Smith, D. K. Neutral Ferrocenoyl Receptors for the Selective Recognition and Sensing of Anionic Guests. *Inorg. Chem.* **1997**, *36*, 2112−2118.
(39) Gavette, J. V.; Mills, N. S.; Zakharov, L. N.; Johnson, C. A.; Johnson, D. W.; Haley, M. M. An Anion-Modulated Three-Way Supramolecular Switch that Selectively Binds Dihydrogen Phosphate, $H_2PO_4^-$. *Angew. Chem., Int. Ed.* **2013**, *52*, 10270−10274.
(40) Kondo, S.-I.; Hiraoka, Y.; Kurumatani, N.; Yano, Y. Selective recognition of dihydrogen phosphate by receptors bearing pyridyl moieties as hydrogen bond acceptors. *Chem. Commun.* **2005**, 1720−1722.
(41) Kondo, S.; Takai, R. Selective Detection of Dihydrogen Phosphate Anion by Fluorescence Change with Tetraamide-Based Receptors Bearing Isoquinolyl and Quinolyl Moieties. *Org. Lett.* **2013**, *15*, 538−541.
(42) Kwon, T. H.; Jeong, K.-S. A molecular receptor that selectively binds dihydrogen phosphate. *Tetrahedron Lett.* **2006**, *47*, 8539−8541.
(43) Gong, W.; Bao, S.; Wang, F.; Ye, J.; Hiratani, K. Two-mode selective sensing of $H_2PO_4^-$ controlled by intramolecular hydrogen bonding as the valve. *Tetrahedron Lett.* **2011**, *52*, 630−634.
(44) Král, V.; Furuta, H.; Shreder, K.; Lynch, V.; Sessler, J. L. Protonated Sapphyrins. Highly Effective Phosphate Receptors. *J. Am. Chem. Soc.* **1996**, *118*, 1595−1607.
(45) Kubik, S. Anion Recognition in Water. *Chem. Soc. Rev.* **2010**, *39*, 3648−3663.
(46) Pitzer, K. S. Thermodynamics of Electrolytes. I. Theoretical Basis and General Equations. *J. Phys. Chem.* **1973**, *77*, 268−277.
(47) Debye, P.; Hückel, E. On the Theory of Electrolytes. I. Freezing Point Depression and Related Phenomena. *Phys. Z.* **1923**, *9*, 185−206.
(48) Davies, C. W. The Extent of Dissociation of Salts in Water. Part VIII. An Equation for the Mean Ionic Activity Coefficient of an Electrolyte in Water, and a Revision of the Dissociation Constants of Some Sulphates. *J. Chem. Soc.* **1938**, 2093−2098.
(49) Brezonik, P. L. *Chemical Kinetics and Process Dynamics in Aquatic Systems*, 1st ed.; CRC Press: Boca Raton, FL, 1993; pp 155ff.
(50) Hamer, W. J. Theoretical Mean Activity Coefficients of Strong Electrolytes in Aqueous Solutions from 0 to 100 °C. National Standard Reference Data Series-National Bureau of Standards 24 (NSRDS-NBS 24). U.S. Government Printing Office: Washington, DC, 1968; pp 2−9.
(51) Butler, J. N. *Ionic Equilibrium: Solubility and pH Calculations*; Wiley Interscience: New York, 1998; pp 41ff.
(52) Manov, G. G.; Bates, R. G.; Hamer, W. J.; Acree, S. F. Values of the Constants in the Debye-Hückel Equation for Activity Coefficients. *J. Am. Chem. Soc.* **1943**, *65*, 1765−1767.
(53) Perrin, D. D.; Dempsey, B. *Buffers for pH and Metal Ion Control*; Wiley: New York, 1974; pp 6−7.
(54) *CRC Handbook of Chemistry and Physics*, 89th ed.; Lide, D. R., Ed.; CRC Press: Boca Raton, FL, 2008; Section 8.
(55) Perrin, D. D. *Ionisation Constants of Inorganic Acids and Bases in Aqueous Solution*, 2nd ed.; Pergamon: Oxford, U.K., 1982.
(56) Daniele, P. G.; Rigano, C.; Sammartano, S. Ionic Strength Dependence of Formation Constants 1. Protonation Constants of Organic and Inorganic Acids. *Talanta* **1983**, *30*, 81−87.
(57) Horn, F.; Jackson, R. General Mass Action Kinetics. *Arch. Ration. Mech. Anal.* **1972**, *47*, 81−116.
(58) Dickenstein, A.; Millán, M. P. How Far is Complex Balancing from Detailed Balancing? *Bull. Math. Biol.* **2011**, *73*, 811−828.
(59) Wu, J.; Vidakovic, B.; Voit, E. O. Constructing Stochastic Models from Deterministic Process Equations by Propensity Adjustment. *BMC Syst. Biol.* **2011**, *5*, 187−208.
(60) Osborn, D. L. Reaction Mechanisms on Multiwell Potential Energy Surfaces in Combustion (and Atmospheric) Chemistry. *Annu. Rev. Phys. Chem.* **2017**, *68*, 233−260.
(61) Tyson, J. J.; Novak, B. Regulation of the Eukaryotic Cell Cycle: Molecular Antagonism, Hysteresis, and Irreversible Transitions. *J. Theor. Biol.* **2001**, *210*, 249−263.
(62) Berninger, J. A.; Whitley, R. D.; Zhang, X.; Wang, N.-H. L. A Versatile Model for Simulation of Reaction and Nonequilibrium

DOI: 10.1021/acs.jced.8b00146
J. Chem. Eng. Data XXXX, XXX, XXX−XXX

Dynamics in Multicomponent Fixed-Bed Adsorption Processes. *Comput. Chem. Eng.* **1991**, *15*, 749−768.
(63) van der Linde, S. C.; Nijhuis, T. A.; Dekker, F. H. M.; Kapteijn, F.; Moulijn, J. A. Mathematical Treatment of Transient Kinetic Data: Combination of Parameter Estimation with Solving the Related Partial Differential Equations. *Appl. Catal., A* **1997**, *151*, 27−57.
(64) Wolfram Mathematica 9.0 Documentation Center, Wolfram Research Inc. http://reference.wolfram.com/mathematica/ref/NDSolve.html (accessed Feb 23, 2016).
(65) *Mathematica, Version 9.0*; Wolfram Research, Inc.: Champaign, IL, 2012.
(66) Shibata, M.; Sakaida, H.; Kakiuchi, T. Determination of the Activity of Hydrogen Ions in Dilute Sulfuric Acids by Use of an Ionic Liquid Salt Bridge Sandwiched by Two Hydrogen Electrodes. *Anal. Chem.* **2011**, *83*, 164−168.
(67) Atkins, P.; de Paula, J. *Physical Chemistry*, 7th ed.; W. H. Freeman: New York, 2002; pp 258, 962.
(68) Ganesh, K.; Soumen, R.; Ravichandran, Y. Janarthanan. Dynamic Approach to Predict pH Profiles of Biologically Relevant Buffers. *Biochem. Biophys. Rep.* **2017**, *9*, 121−127.
(69) DaSilva, J. A.; Barría, C. S.; Jullian, C.; Navarrete, P.; Vergara, L. N.; Squella, J. A. Unexpected Diastereotopic Behaviour in the 1H NMR Spectrum of 1,4-Dihydropyridine Derivatives Triggered by Chiral and Prochiral Centres. *J. Braz. Chem. Soc.* **2005**, *16*, 112−115.
(70) Platzer, G.; Okon, M.; McIntosh, L. P. pH-Dependent Random Coil ^{1}H, ^{13}C, and ^{15}N Chemical Shifts of the Ionizable Amino Acids: A Guide for Protein pK_a Measurements. *J. Biomol. NMR* **2014**, *60*, 109−129.
(71) Lee, L. L. *Molecular Thermodynamics of Electrolyte Solutions*; World Scientific: Hackensack, NJ, 2008; pp 39−49.

DOI: 10.1021/acs.jced.8b00146
J. Chem. Eng. Data XXXX, XXX, XXX−XXX